Jour. Ind. Geol. Cong., Vol.6(1),
June 2014, pp.35-46.

Geotechnical Applications of Ground Penetrating Radar (GPR)

B. Venkateswarlu and Vinod C. Tewari
National Geotechnical Facility, 11/c, Circular Road, Dalanwala, **Dehradun** - 248 001
Wadia Institute of Himalayan Geology (WIHG),
Dehradun - 248 001 (Uttarakhand)
Emails : *bvenkatiitd@gmail.com; vtewari@wihg.res.in*

Abstract : A Ground Penetrating Radar (GPR) applications in the earth science has been reviewed. The fundamentals of the GPR technique and potentialities of the GPR applications in the field of geotechnical engineering are explained in this review paper . Penetration depth and vertical resolution depend on the soil conditions, characteristics of input signal and configuration of the transmitter–receiver assembly. GPR has shown to be a viable approach due to the facts that it has proven to use in wide-range of applications in the field of geo-engineering such as detection of soil and rock profiling, water-table detection and bedrock identification, identifying structural features in subsurface, and bars checking in reinforcement and beam columns. Depending upon targeted object central frequency of antenna have to be selected appropriately so as to get better resolutions of reflection profile which is to be studied in detail. Different GPR central frequencies antennas results are reviewed in this paper such as 250 MHz, 300MHz, 500 MHz and 1 to 6 GHz. The results show that the 250 MHz GPR had a low resolution and higher depth penetration, while the high frequency 1 to 6 GHz GPR antennas has a shallow detecting depth with high resolution. In estimating geological structural features such as cracks, fractures and joints, etc., are very important to assess the potential detection of natural hazards. GPR has been viable technique in mapping structural features (Fig.14) and also it has got extended capabilities of mapping extension and continuity of these structural features. GPR has also confirmed that the electromagnetic waves are most strongly reflected by cracks containing air or water or clay content. Internal structures of cement structure layers are viable to identify with better resolutions as shown in Fig.17 and Fig.19. Fig.17 shows a reflection radar profile of concrete slab with 10 mm re-bars at different depth levels and also contrast against thickness of concrete slab can be observed. From this figure it clearly demonstrates the ability of such high-frequency radar antennas to map re-bars with sub-centimeters accuracy. In order to satisfy requirements for detection of subsurface objects and better resolution repeated survey would be performed on the selective/anomalous site, so as to remove false phenomena resulted from bumping of GPR antenna or interference from ground objects.

Keywords : Ground Penetrating Radar, Geotechnical, Electromagnetic waves, Subsurface structures, Reflection profile, Polar ice echo radio sounding.

INTRODUCTION

Geophysical methods are proved to be powerful tools in the study of the Earth. In the last two decades, ground penetrating radar (GPR) is one among geophysical methods that has been employed increasingly in many scientific and engineering disciplines for a variety of applications. By exploiting the wave propagation characteristics of electromagnetic fields, GPR provides a very high resolution sub-surface mapping information to a depth of typically 0 to 10 m, although depths up to 40 m (Franke &Yelf, 2003; Jol, 2003; Bakker, 2004) are possible in some geological environments. GPR in its present form started to emerge from the polar ice radio echo sounding in the late 1960s. Since that time, the method has seen constant and continuous growth both in applications, number of users and instrument sophistication. The first use of GPR signals to determine the presence of remote terrestrial metal objects is generally attributed to Hulsmeyer (1904), but the first description of their use to locate buried objects only appeared six years later in a German patent by Leim bachand Lowy (1910). Early utilization of this method for engineering applications were given by Morey (1974), Annan and Davis (1976), and Ulriksen (1982). Ground Penetrating Radar (GPR) was designed primarily to locate objects or interfaces buried beneath the earth's surface (Daniels et al., 1988). The pulsed radar has been developed and being used commercially extensively for the past two decades in many applications e.g. in determination of the ice thickness (Walford,1985; Evans et al.,1988), in permafrost measurements (Annan and Davis, 1976), in civil engineering (Morey, 1974), in overburden characterization (DavisandAnnan,1989), in peat surveys (Ulriksen, 1982), in salt deposit measurements (Thierbach, 1974; Unterberger, 1978) and in coal-seam probing (Coon et al., 1981; Ralston, 2000). Furthermore the range of applications have been expanding steadily, and now includes archaeology, road and rail bed quality assessment, location of voids, tunnels and land mines etc. location of underground tunnels and voids (Olhoeft, 1988; Moran and Greenûeld, 1993). Applications of this technique include delineation of ore bodies (Fullagar et al., 2000); mapping fractures in bedrock (Olsson et al., 1992; Day-Lewis et al., 2003); and estimation of subsurface lithology and hydrogeologic properties using ûeld- or laboratory-derived petro physical relationships (Alumbaugh and Chang, 2002; Moysey and Knight, 2004; Tronicke et al., 2004). The recent advances of the use of GPR for the investigation of sediments can be found in Bristow and

Jol (2003) and Bristow (2004). Recently, several studies have proven GPR to be instrumental in analyzing near surface earth structures (Yetton and Nobes, 1998; Veeken et al., 1999; Gross et al., 1999 and 2000; Salvi et al., 2003; Al-Shukri et al., 2006).

In this paper, principle of GPR and its applications to geo-engineering has been examined such as subsurface profiling, water-table detection and bedrock identification, identifying structural features in subsurface, and bars checking in reinforcement and beam columns. New instrumentation has significantly improved the ability to rapidly collect deep and high resolution GPR data in a variety of environments, thereby expanding the capabilities of the GPR.

GPR PRINCIPLE

Ground penetrating radar produces a continuous cross-sectional profile or record of subsurface features, without drilling, probing, or digging. GPR operates by transmitting pulses of ultra high frequency electro-magnetic (EM) waves down into the ground through a transmission antenna. When the transmitted signal enters the ground, it contacts objects or subsurface strata with different electrical conductivities and dielectric constants. A certain amount of energy is reflected and picked-up by a receiving antenna, the remaining energy continue to pass into the ground to be further reflected, until it finally spreads and dissipates with depth as shown in Fig. 1. The control unit registers the reflections against two-way travel time in nanoseconds and then amplifies the signals. The output signal voltage peaks are plotted on the GPR profile as different colour bands by the digital control unit.

Ground penetrating radar waves can reach depths up to 100 feet (30 meters) in low conductivity materials such as dry sand or granite. The depth range of GPR is limited by the electrical conductivity of the ground, the transmitted center frequency and the radiated power. As conductivity increases, the penetration depth decreases. This is because the electromagnetic energy is more quickly dissipated into heat, causing a loss in signal strength at depth. Higher frequencies do not penetrate as far as lower frequencies, but give better resolution.

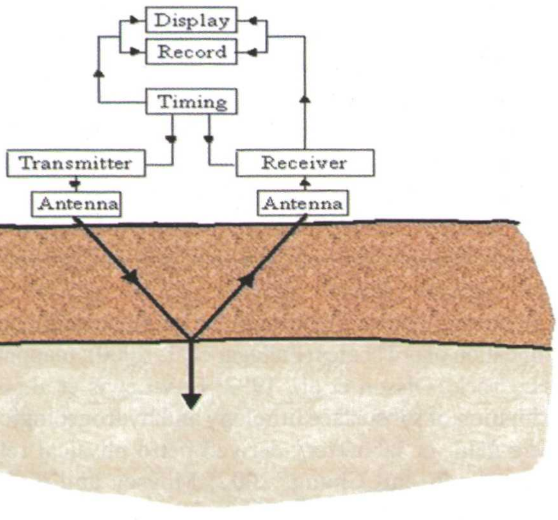

Fig.1. Schematic diagram of a ground-penetrating radar system.

Dielectric constant 'ε' is a number that relates the ability of a material to carry alternating current to that of vacuum. The relationship between dielectric constant 'ε' and the EM wave velocity 'v' can be expressed as (Ulbay, 2007).

$$v \quad \frac{c}{\sqrt{\varepsilon}} \qquad \text{Eq. 1}$$

Where: 'c' is the velocity of the EM waves in vacuum.

The reflection coefficient of the EM waves is defined as (Ulbay, 2007).

$$R_i \quad \frac{\sqrt{\varepsilon_{i\ 1}} - \sqrt{\varepsilon_i}}{\sqrt{\varepsilon_{i\ 1}} + \sqrt{\varepsilon_i}} \qquad \text{Eq. 2}$$

Where R_i is the reflection coefficient of the EM waves propagating from medium 'i-1' to medium 'i', and ε_{i-1} and ε_i are the dielectric constants of media i-1 and i, respectively. If the absolute value of R_i is greater than zero, meaning there is a dielectric property difference between the two media, reflection will then occur on the boundary. The dielectric constant 'ε' not only determines the EM wave velocity 'v' of a certain medium, but also governs the reflection characteristics of the boundary. Therefore, the dielectric constants of all detecting materials are needed for a proper analysis of the GPR data.

ANTENNA VARIABLES

One of the most important variables in GPR surveys is the selection of antennas with the correct operating frequency for the depth necessary and the resolution of the features of interest (Huggenberger et al., 1994; Smith and Jol, 1995). Commercial GPR antennas used in most archaeological applications range from 10 to 1500 MHz frequency (Annan and Cosway, 1994; Fenner, 1992; Malagodi et al., 1996; Olson and Doolittle, 1985; Jol and Bristow, 2003). General purpose GPR systems use dipole antennas that typically have a two-octave band width, meaning that the frequencies vary between one half and two times the central frequency.

Most important, just because a manufacturer identifies an antenna as having one frequency, doesn't necessarily mean that it will produce radar energy with a center at exactly that frequency. A primary goal of all antenna manufacturers is to produce a clean pulse of one wavelength in duration that can be transmitted into the ground. No antennas, however, produce perfectly clean pulses, and somewhat noisy reflection records generated from noisy transmitted pulses are always the norm.

Proper antenna centre frequency selection, in most cases, makes the difference between success and failure of a GPR survey, and must be planned for in advance. Lower-frequency antennas are for the most part much larger, heavier, and more difficult to transport within the field than high-frequency antennas. Larger, lower-frequency antennas are more difficult to shield and therefore have the potential to receive many extraneous reflections from surface objects, and they can thus be quite "noisy". However, smaller, higher-frequency antennas are usually shielded, which allows energy propagation downward into the ground, but not upward or to the sides where it could be reflected off surface features, the antenna cables, or even the people pulling the antennas (Lanz et al., 1994).

Table 1. Radar pulse width and depth resolutions for various central frequencies and Relative Permittivities (ε_r).

Central frequency (MHz)	Pulse-width (ns)	Depth resolution in cm	
		ε_r=4 sandy dry soil	ε_r=15 (sandy wet soil)
100	6.4	75	38.0
500	2	15	7.7
1000	1	7.5	3.9
1500	0.75	5	2.6
2000	0.5	3.75	1.9
3000	0.33	2.5	1.3

As discussed above, the choice of the central frequency and bandwidth of the GPR is an important issue, and it depends primarily on the type of application in the field. For each application a different set of frequency antenna constraints can be developed. The parameters influencing the frequency range are : depth of maximum penetration depth, size of the object, wanted-depth resolution and properties of the study area.

In conclusion, for good depth resolution, short pulses are needed, which means larger bandwidth. With refer to the above Table 1; we saw that the depth of penetration strongly decreases with higher frequencies for a given soil. The electrical properties of the soil together with the wanted maximum depth penetration imply an upper limit for the used frequencies. Once frequencies above 1 GHz are used, depth penetration decreases dramatically. So if large penetration depth is needed, lower frequencies are preferred.

As a general rule, it is desirable that the wavelength of the central frequency in the ground of the GPR is ten times larger than the size of the heterogeneities in the ground.

RADAR DATA ACQUISITION MODES

GPR data acquisition can either be used in reflections or transmission modes. In reflection mode of surveys there are few different techniques and is normally conducted using two antennae (called the bi-static mode), with a separate transmitter (T_x) and receiver (R_x) as shown in Fig.2(a). Transmission survey mode can be used to obtain more detailed sub-surface tomography profile between the two bore holes as shown in Fig.2(b). There are four main modes of radar data acquisition in reflection and transmission techniques, namely: Common offset (Reflection profiling), Wide-angle reflection and refraction (WARR), Common midpoint sounding (CMP), and Cross-hole radar tomography or Trans-illumination.

Common Offset Profiling

A profile is a graph of a measured quantity against horizontal distance. In this mode of operation, the radar transmitter (T_x) and receiver (R_x) antennae are moved over the surface simultaneously. The measured travel times to radar reflectors are displayed on the vertical axis, while the distance the antenna has travelled is displayed along the horizontal axis in a radar gram display. Most GPR surveys, mainly borehole radar surveys use a common offset survey mode. Fig.3 shows a common offset bi-static mode data acquisition configuration.

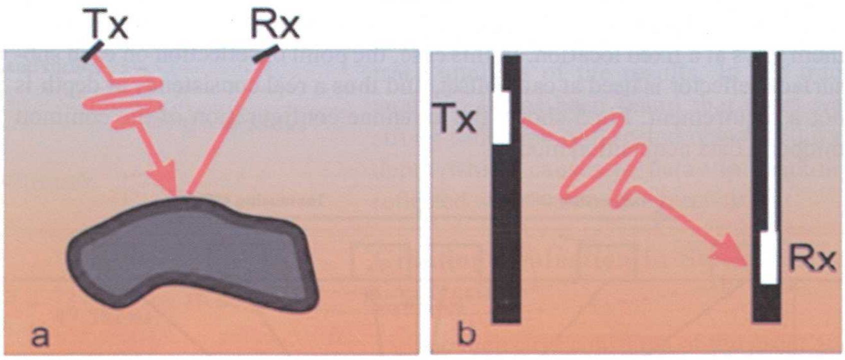

Fig.2. GPR reflection and transmission.

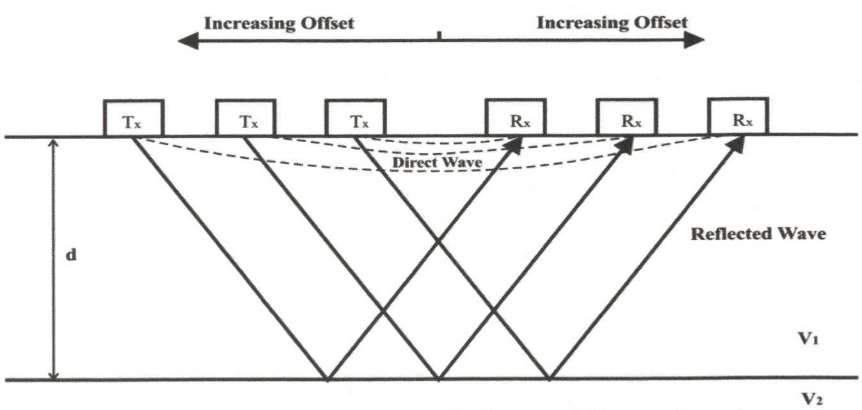

Fig.3. Common offset bi-static mode data acquisition configuration.

Wide-Angle Reflection and Refraction (WARR)

In a common source data acquisition system, sometimes called wide-angle reflection and refraction (WARR) sounding (Reynolds, 2000), the transmitter (T_x) is kept at a fixed location and the receiver (R_x) is lowed away at increasing offsets. Fig.4 shows the antennae conûguration of a common source data acquisition mode. This type of data acquisition mode is most suitable in an area where the material properties are uniform and the reflectors are planar in nature.

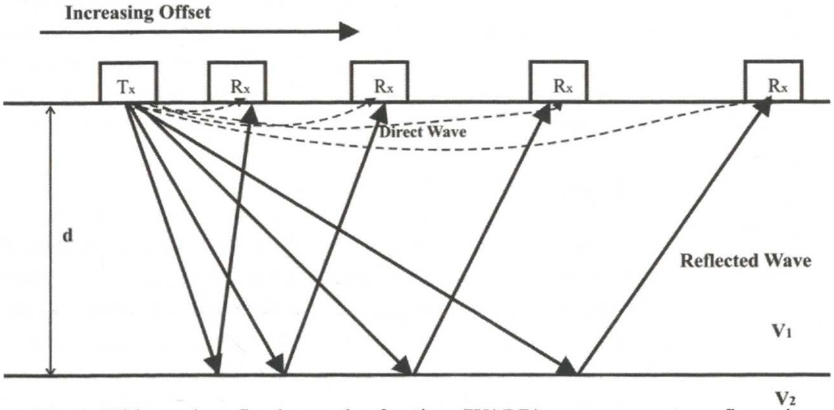

Fig.4. Wide-angle reflection and refraction (WARR) measurement configuration.

Common Midpoint Sounding (CMP)

In this type of acquisition mode, the transmitter (T_x) and receiver (R_x) antennae are moved away at increasing offsets so that the midpoint between them stays at a fixed location. In this case, the point of reflection on each sub-surface reflector is used at each offset, and thus a real consistency at depth is not a requirement. Fig.5 shows the antennae configuration of the common midpoint data acquisition mode.

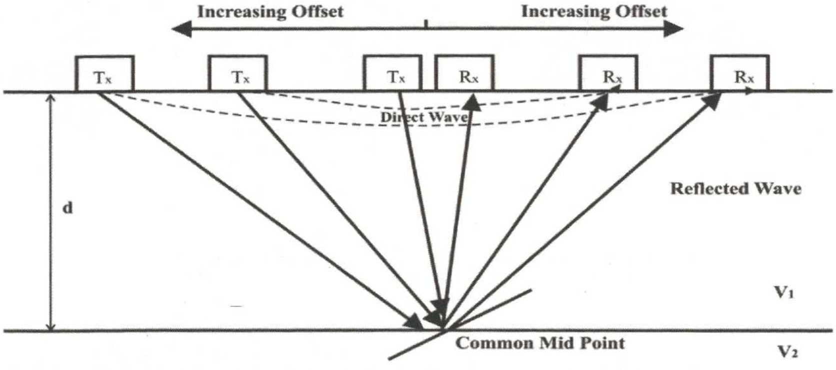

Fig.5. Common midpoint (CMP) measurement configuration.

Cross-Hole Radar Tomography or Trans-Illumination

In the transmission mode of deployment, the transmitter (T_x) and receiver (R_x) antennae are on opposite sides of the medium being investigated. This type antenna of configuration, as shown in Fig.6, is often used in underground mines and Dams. As the relative positions of the radar antennae are known at all times, and hence the distances between them, the mean radio wave velocity can be derived from the time section. More details of this method can be found in Annan and Davis (1977).

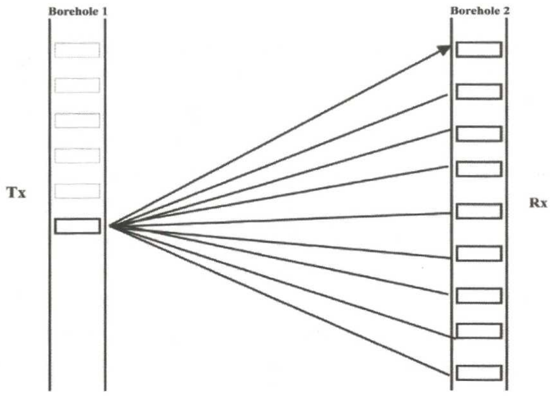

Fig.6. Transmitter and receiver antenna are kept indifferent borehole.

APPLICATIONS OF GPR IN GEOTECHNICAL ENGINEERING

In this study, wide-range of papers have been reviewed in regard to applications of GPR in the field of geo-engineering. It is found that GPR provides a powerful method of subsurface profiling with high resolution of reflection profile. Thereby use of GPR has been extend in widespread areas such as in Pavement, Construction, Utilities detection, Hydrology, Mining, Archaeological, Forensic science, Unexploded Ordnance, Environmental Studies, and Miscellaneous applications like in agriculture, demining (find landmines), graves and burials. Detectable objects can range in size from around 10 mm to underground cavern proportions.

Identification of the Water-Table Reflector

The strength of the water-table radar reflector depends on the contrast between the electrical properties of the unsaturated and saturated zones. In coarse-grained sands the capillary fringe is usually abrupt, especially during dry period, because the pore spaces are large and many are essentially non capillary. The water table reflector is more pronounced in these deposits and the position on the graphic record is relatively easy to locate. In the fine-grained materials, the capillary fringe is more gradual because of the presence of smaller, more continuous pore space, and the water-table is less distinct on the graphic record. Also, where reflective stratigraphic features are close to the water-table, the water-table reflection is less abrupt, or masked by overlapping reflections.

GPR measurements were presented using a physical model that simulates a rising and falling water -table in the earth. The GPR data were collected with antenna having central frequency of 500 MHz. Consistent data acquisition instrument setting on the GPR system was used throughout the experiment in order to reduce and facilitate data processing steps. This investigation was done to determine the depth of water-table in site location. Fig.7 shows the site location where GPR was been carried and drilled four boreholes in the each corner of the site for cross checking with GPR profiling. Fig.8 shows the clear distinguishable reflections from the subsurface to water table. The dielectric constant of the water-table was then determined indirectly based on the electromagnetic wave velocity calculated as shown below in Fig.8 by measuring travel time of the EM waves at water table interface (Mundher et al., 2011).

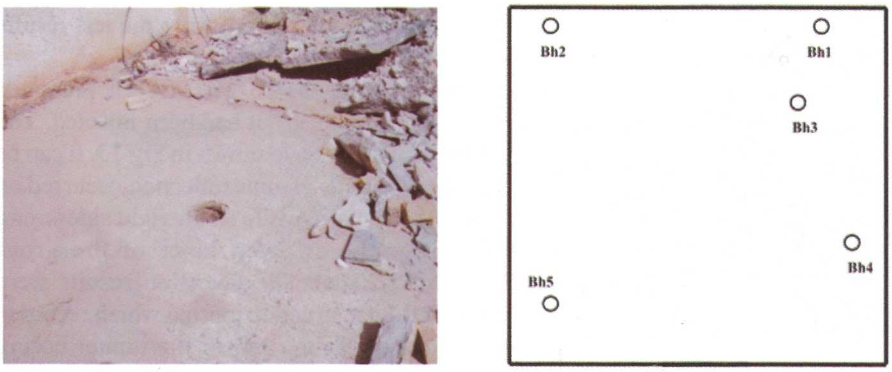

Fig.7. Site map with position of the required boreholes.

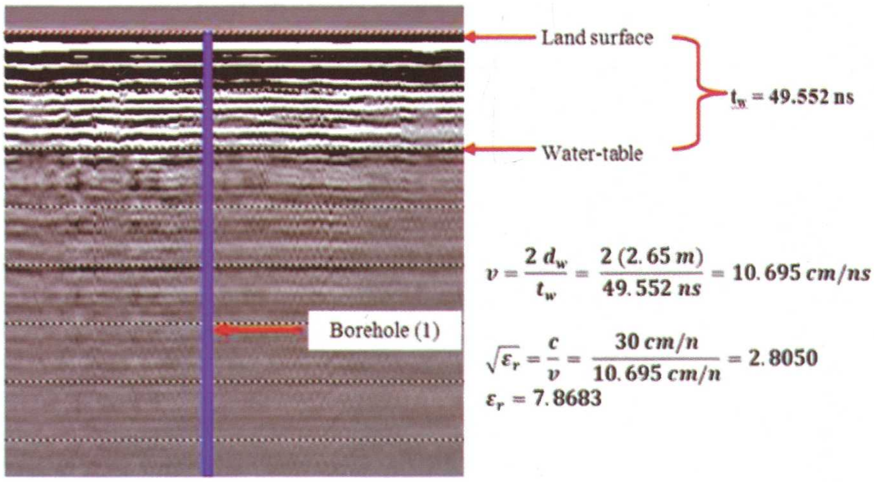

$$v = \frac{2\,d_w}{t_w} = \frac{2\,(2.65\ m)}{49.552\ ns} = 10.695\ cm/ns$$

$$\sqrt{\varepsilon_r} = \frac{c}{v} = \frac{30\ cm/n}{10.695\ cm/n} = 2.8050$$

$$\varepsilon_r = 7.8683$$

Fig.8. GPR profile image across the borehole #1.

Identification of Soil Stratigraphy and Bedrock Depth

The surface topography was surveyed and the data have been corrected for the topographic variations along the survey line (Grandjean et al., 2000). A view of correlation between borehole information and the migrated section as shown in Fig.9 indicated that most of the reflections are related to electromagnetic waves contrasts due to lithology.

The reflection coefficient as soil/rock layers changes from one layer to another shows contrast of electromagnetic waves caused due to changes in dielectric and electrical permittivity constants as highlighted in Fig.10. The data are in a form that is amenable to a wide variety of digital enhancement processing techniques.

Identification of Buried Utilities

Where the locations and depths of distinct underground objects must be determined, GPR is the technique of choice when the host medium permits adequate penetration. At many industrial, commercial, and residential complexes, map layouts showing the distribution of underground utility lines (water, sewer, storm drains, electric, telephone, cable TV, etc.) are often non-existent or inaccurate. Underground utility lines must be located prior to repair or removal. In case, any lack of accuracy in the built drawing layouts/plans in regard of buried utility lines may leads to rupture/damage of water main lined or selected electric conduits with consequent structural damage or injury to personnel during drilling or coring operations.

In the GPR data processing, it shows a strong reflection against the pipeline around at 0.6 m depth from the test results (Olhoeft, 2000) as shown in Fig.11. The same observation was also supported by the single trace analysis of the results. In the trace analysis, it has been found that there was strong reflection of targeted object at 0.6 m depth which causes to delay in reaching reflected wave back to the receiver.

Grouting Evaluation in Shield Tunnel Construction

The dielectric constants of the grout and the soil were determined by the indirect method based on measuring the EM wave travel time through the grout segments was used instead as calculated in above Fig.8. Since the segments were manufactured with a constant thickness of 0.35 m, the EM wave velocity and consequently the dielectric constant can be determined if the EM wave travel time through the segment was known. In order to accurately compute the travel time from the GPR data, a composite system with a metal plate stuck on the outer surface of the lining segments was constructed so as to cause absorption and strong reflection of the EM waves. When the EM waves propagate from one material with a high dielectric constant to another with a low dielectric constant, the reflection coefficient will be positive, according to Eq. (2) given under GPR principle, and no phase reversal will occur. Conversely,

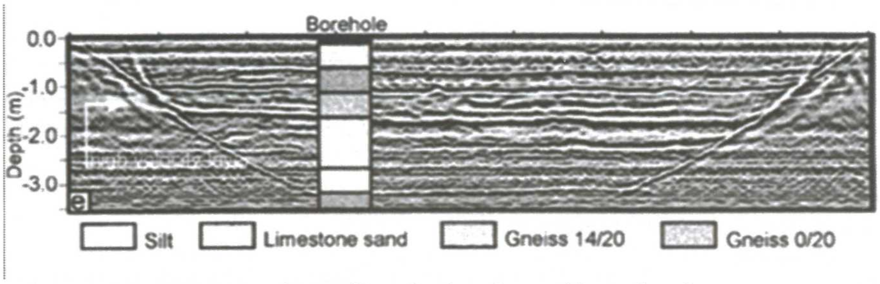

Fig.9. A radar profile reflection along with stratigraphy.

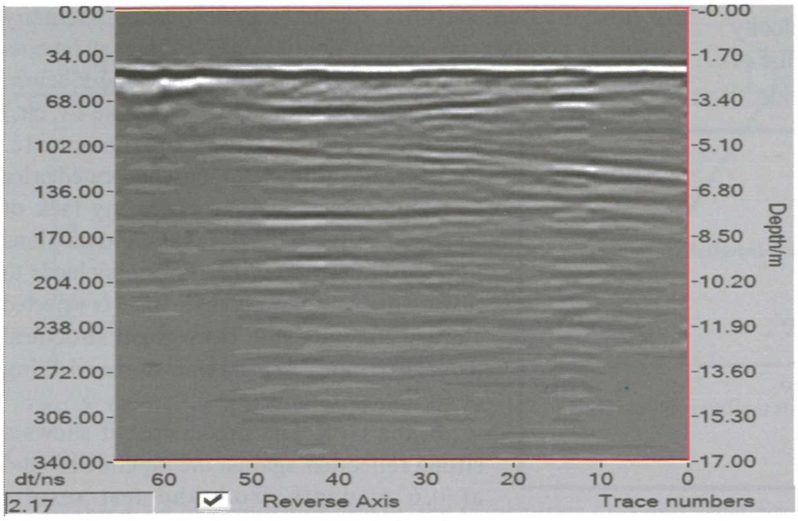

Fig.10. A radar reflection profile showing the stratigraphy.

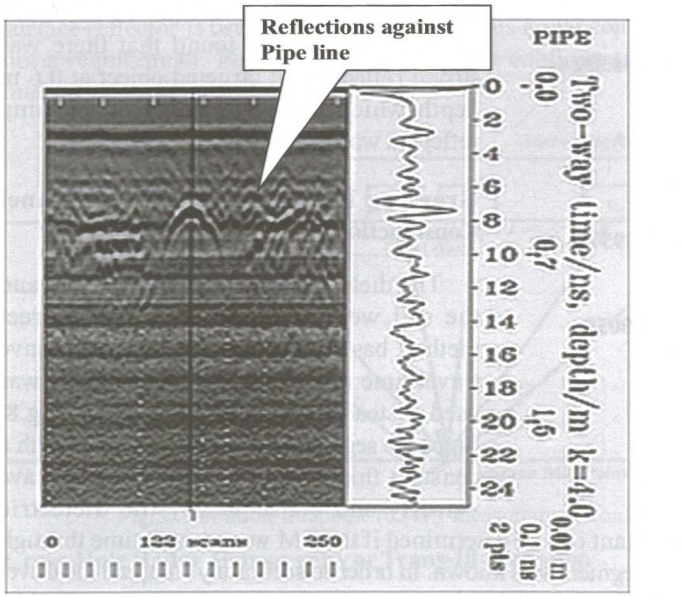

Fig.11. Raw radar data acquired towed across a 90-cm dia pipe buried 37 cm deep.

when the EM waves travel from one material with a low dielectric constant to another with a high dielectric constant, then the reflection coefficient will be negative and phase reversal can be observed.

Frequency of 1 GHz GPR was used to determine the EM wave velocity in the concrete segment. The GPR detection was carried out along the inner surface of a grout lining segment to detect reflected waves (Fig.12). Two different cases can be tested for better understanding the change of reflections in the EM waves. In case 1, metal plate was placed in the outer surface of the lining segment over the whole test area. In case 2, the metal plate can be placed on the inner surface of the lining segment. Case 1 GPR data was processed by MATLAB with proper gain. Strong reflection due to the existence of the metal plate outer surface of the lining segment can be clearly identified (Fengshou et al., 2010) from the test results shown in Figs.12.

Grout detection using the 250 MHz GPR is presented here; one month after the grout had been injected. The processed data of 10 m long is shown in Fig.13. It can be seen from Fig.13 that no obvious reflection occurred on the left side of the domain, while on the right side strong reflection suggested an even layer of the grout (Fengshou et al., 2010). The detection results were consistent with the construction journal which recorded leakage of the grout in the tail of the tunnel boring machine when excavating at the length of 0–5 m.

Identification of Cracks in the Rock

One of the main causes of base rock collapse is called progressive destruction or progressive cracking. Cracks in the base rock progress as a result of weathering of the rock and lead to base rock collapse. It is very important to know the continuity and distribution of cracks inside the base rock as well as the extent of surface cracking to estimate the danger of collapse.

The GPR technique utilizes electromagnetic (EM) waves to provide useful resolution and non-destructive measurements of dielectric contrasts in geological materials and formations. When a crack contains clay or water, it becomes a strong reflector of EM waves because of the sharp contrast in velocity between the crack and the surrounding rock (Ulriksen, 1982).

In regard to the part above, 300 MHz shield antenna was utilized to satisfy requirements for detection depth and resolution. In the process of detection, if there appears any anomaly in GPR images for the sloping clay core, then repeated detection would be performed on the anomalous site, so as to remove false phenomena resulted from bumping of GPR antenna or interference from ground objects.

In response to the GPR survey, three sampled sites showing linear anomaly (A, B and C in Fig.14), with one area showing strong reflection (D in Fig.14). Cracks were discovered at the three sites showing the linear anomaly, while a fracture zone was discovered in the area showing strong reflection, indicating that

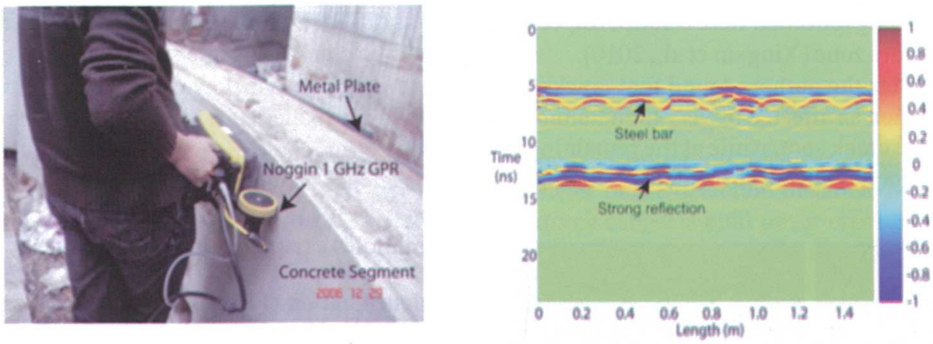

Fig.12. GPR setup with metal plate outside the segment and reflected waves.

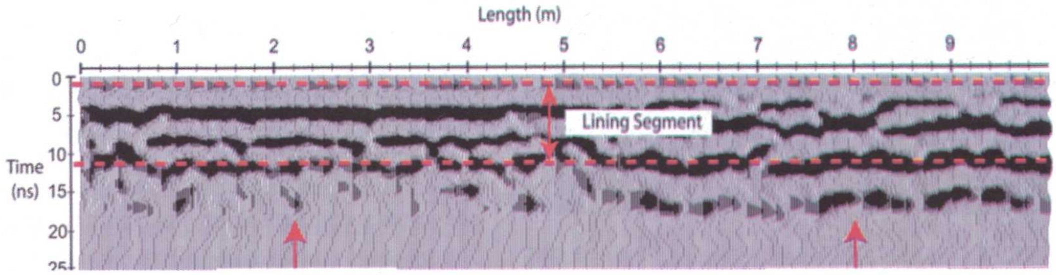

Fig.13. Data of 250 MHz GPR field test.

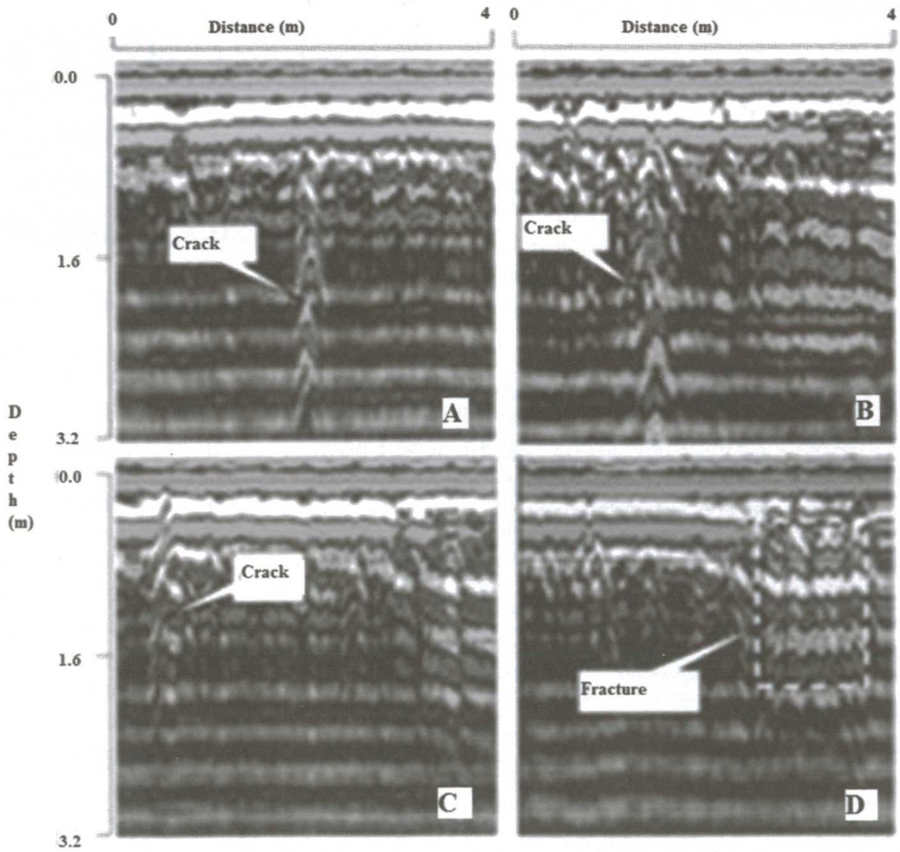

Fig.14. GPR images showing cracks and a fracture zone in sloping clay core.

the linear anomaly and strong reflection were resulted respectively from the cracks and fracture zone (Xingxin et al., 2010).

At the excavation sites, the authors found that cracks were closed due to soil expansion as affected by very high humidity at the fracture zone and one crack spot, while at the remaining two crack spots, cracks can be vividly seen inside the sloping clay core (Fig.15).

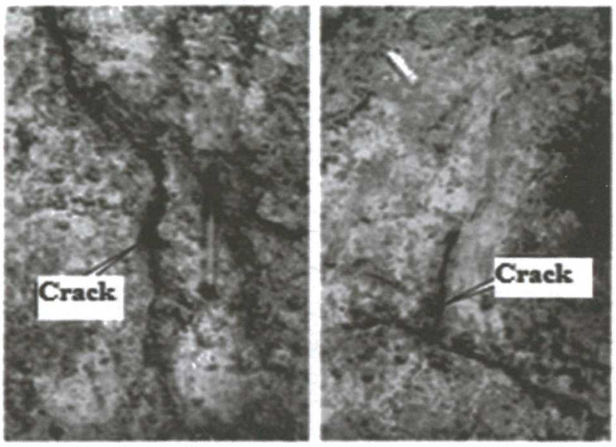

Fig.15. Photos showing excavation of cracks inside a sloping clay core for corroboration.

Therefore, it can be inferred that GPR technique is capable of detecting rock structural features such as cracks, fractures, Faults and Folds etc.

Identification of Subsidence and Cavity

A study of the GPR traverse shown in Fig.16 was recorded as an example (across US Highway 6 near the Eureka, Juab County, Utah). Two areas of apparent subsidence in the upper strata can be seen in Fig.16. Any surface expressions of this slumping were most likely filled in many years ago when the highway was resurfaced. Some nearby cracking and warping in the highway may be clues that some subsurface movement is still occurring. Almost directly below each area of subsidence is a hyperbolic diffraction pattern that is characteristic of reflections from localized objects or cavities in the sub-surface (Benson, 1995). The hyperbolae in Fig.16 most likely originate from man- made cavities, such as a mine shaft or a tunnel, but could also arise from sinkholes carved out in the limestone.

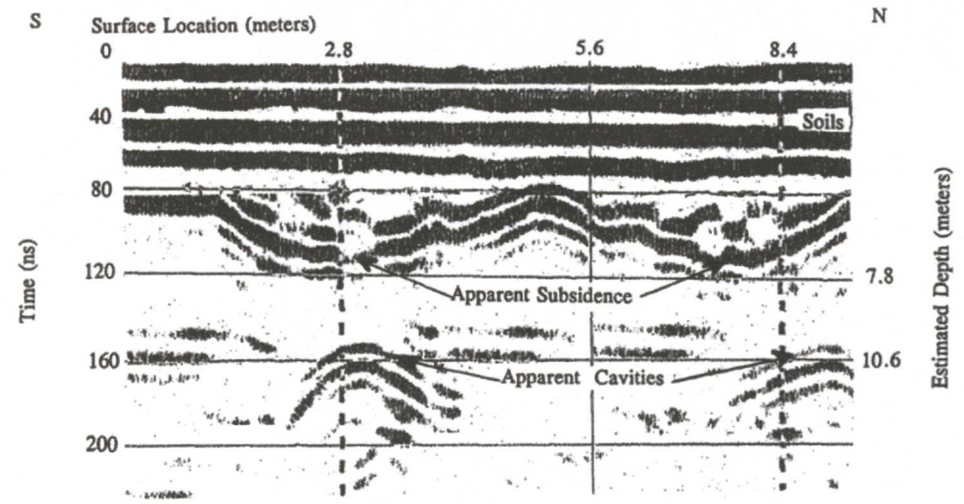

Fig.16. GPR Profile (across US Highway 6, near Eureka, Juab County, Utah) reflections of subsidence and cavities.

Identification of Re-Bars

GPR can be used successfully as a mapping and non-destructive testing tool for checking of building materials, reinforcement and void space in concrete slabs. Concrete changes its electrical properties as it hardens. Wet concrete has relatively high conductivity and consequently the radar attenuation is high and the detection range is low. In dry concrete however, the range is improved and the high frequency GPR can then be used as a mapping tool for internal structure.

Internal structure may be layers or objects such as cavities, re-bars and pipes. Fig.17 shows a high frequency (1-6 GHz) radar section of a concrete slab with 10mm re-bars at different depths, 2 cm, 4 cm, 6 cm, 8 cm and 10 cm (Kong et al., 1999). Below figure clearly demonstrates the ability of such high-frequency radars to map re-bars with sub-centimetres accuracy.

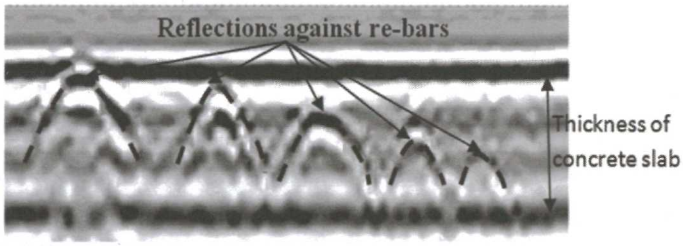

Fig.17. High frequency (6 GHz) radar detecting re-bars in concrete.

Case Studies in NGF Campus

Few case studies of GPR survey carried with in NGF campus :

Detection of re-bars in Concrete Slab

An antenna of 1.5 GHz central frequency with frequency range of 800 to 3000 MHz was used for detection of re-bars in the concrete slab (Fig.18). When antenna moved along re-bars direction in the slab, it is found that continuous reflection of waves observed against the re-bar as highlighted in Fig.19 gray scale plot. However, other part of reflection profile shows a contrast of EM waves

Fig.18. Survey set up of concrete slabs.

at three distinct points as marked in Fig.19 gray scale plot since antenna moved perpendicular to re-bars in the slab (Fig.18). The same observations can be made in colour plot.

Detection of Masonry Brick Wall & Concrete Layer Thickness

In the given Fig.20 on next page shows a reflection profile against thickness of the masonry wall. As stated in the GPR methodology, dielectric constant is the main factor to distinguish any object or stratigraphy layers in reflection profiles. Therefore, higher reflection coefficient results in clear understanding of targeted object. In below GPR reflection profile it is observed that there is a clear band of dark like which represents the thickness of masonry brick wall. Since the change in dielectric constant value between wall and air is quite enough to have better contrast. Antenna of 1.5 GHz central frequency was used with 2 *10 m cable and the measured masonry brick wall thickness from GPR reflection profile is 18 to 20 cm as observed in Fig.20. However another survey carried out on tiled ground crossing canal across the survey line using same antenna. Fig.21 shows strong reflections from trace no 35 to 50 due to an existence of canal across the survey line and also can be seen thickness of concrete layer below the tiled ground.

PRACTICAL PROBLEMS IN FIELD TESTS

a. Power and Amplifier

Network analyzer switches off internal amplifier, when input power is too big.

Don't make antennas too close to each other when amplifier is on.

b. Cable Length and Position

The transmitter and receiver cable length should be bigger than twice of the detection distance. Moreover, while carrying out survey cables should never cross each other.

Cable radiates power. It is important to lay down the cable, at least 3 to 5 m from antennas, on the ground and let ground to absorb the current flowing outside of the cable.

c. Antenna Positions

Antenna separation should be smaller than the smallest detection distance. In-line antennas have smaller direct wave, but the width of the wave is wider. Parallel antennas have larger direct wave, but the width of the wave is narrower. Antenna conductor should be in the same direction to a metal target (re-bars etc.)

CONCLUSIONS

With the objective of studying the applicability of GPR in the field of Geotechnical Engineering, we conducted GPR literature review study, as a result, the following few interpretations and conclusions are drawn :

a. The performance of GPR as a high-resolution subsurface mapping tool has been confirmed by looking at the above examples. Higher the antenna frequency, better the resolutions and less the depth of penetration. In case of detecting re-bars and identifying thickness of concrete layer, high frequency antennas are used and able to trace re-bars locations ant its depth, and thickness of concrete layer.

b. In non-conductive and homogeneous ground conditions, GPR performs very well and detailed pictures of the

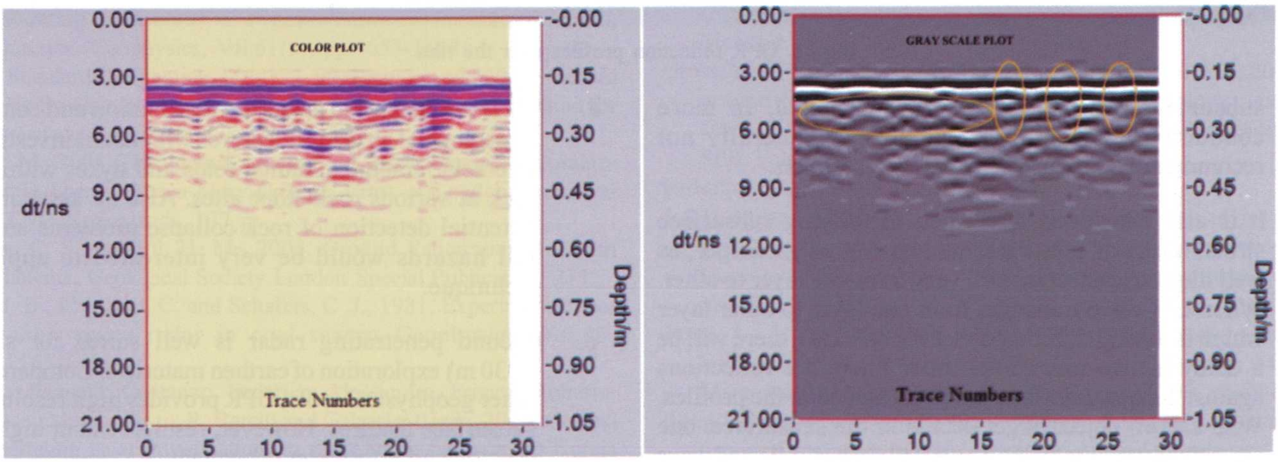

Fig.19. GPR reflection profile against concrete slab.

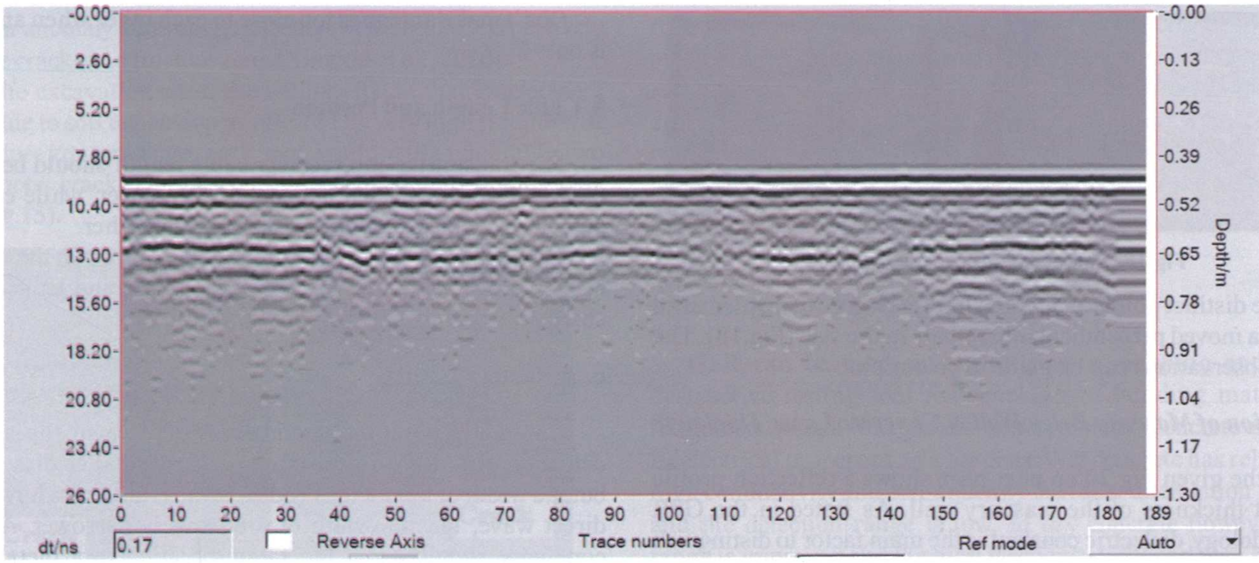

Fig.20. GPR reflection profiles against the concrete wall.

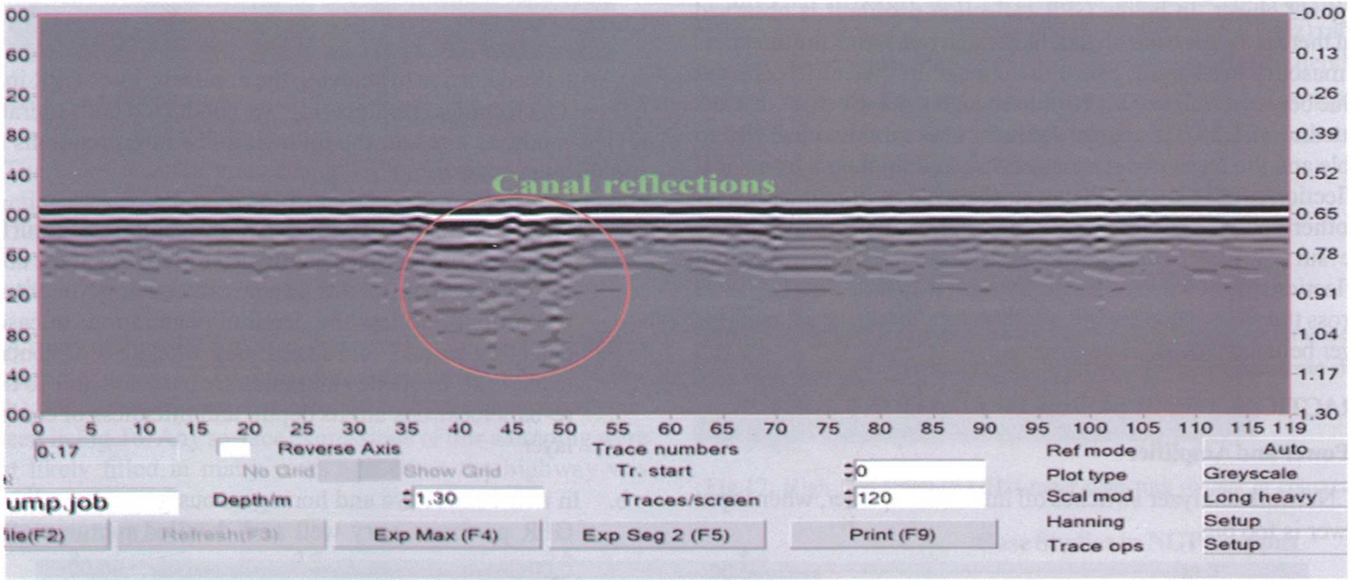

Fig.21. GPR reflection profiles over the tiles.

subsurface profiles can be reconstructed. In more conductive materials this method is generally not recommended because of very low resolution.

c. It is also concluded that when identifying subsurface strata, layers of subsurface will change as go deeper; as well dielectric constant will vary from one layer to other. When EM wave transmits from one layer to other layer which is having different dielectric constant, there will be a delay in two-way travel time. Therefore reflections against the new interface can be identified in the profiles. With known object/target details in the subsurface, one can actually calibrate two way travel time of reflected wave and it's dielectric constant using an indirect method (refer Fig.8).

d. GPR can be used to detect the distribution and continuity of geological structural features with detail investigation of cracks, fractures, faults, folds and dykes within base rock at various rock slope sites. Also an assessment of potential detection of rock collapse problems and rock fall hazards would be very interested to apply this technique.

e. Ground penetrating radar is well suited for shallow (< 30 m) exploration of earthen materials. Compared with other geophysical tools, GPR provides high resolution of subsurface features. However, results remain highly site specific and interpreter dependent.

f. The GPR method, which in favourable conditions is today's most superior shallow subsurface mapping tool, will continue to develop fast, resulting in cheaper equipment, faster data acquisition rates and improved data quality

In summary, in appropriate geology, GPR surveys can provide useful cost-effective data which can help assess potentially dangerous geological hazards. Planning and remedial measures based upon these data can then be implemented.

ACKNOWLEDGEMENTS

We are thankful to Prof. A. K. Gupta, Director, Wadia Institute of Himalayan Geology, Dehradun for encouragement and providing laboratory facilities of the National Geotechnical Facility (DST Project) under Wadia Institute. Prof. O. P. Varma, Executive President and Chief Editor, Journal of Indain Geological Congress is thanked for reviewing the paper and valuable suggetions in its improvement. We are grateful to the anonymous referee for critical review of the paper and encouraging comments for its publication.

REFERENCES

Al-Shukri, Haydar; Mahdi, Hanan, H. and Tuttle, Martitia, 2006. Three-Dimensional Imaging of Earthquake-induced Liquefaction Features with Ground Penetrating Radar near Marianna, Arkansas, Seismo. Res. Lett., Vol.77, pp.505-513.

Alumbaugh, D. and Chang, P. Y., 2002. Estimating moisture contents in the vadose zone using cross-borehole ground-penetrating radar: A study of accuracy and repeatability. Water Resources Research, Vol.38, 1309 p., doi: 10.1029/2001WR000754.

Alvin, K. B., 1995. Applications of ground penetrating radar in assessing some geological hazards: examples of groundwater contamination, faults, cavities. Journal of Applied Geophysics, Vol.33, pp.177-193.

Annan, A. P. and Davis, J. L., 1976. Impulse radar sounding in permafrost. Radio Sci., Vol.11, pp.383-394.

Arcone, S. A., 1996. High resolution of glacial ice stratigraphy: A ground-penetrating radar study of Pegasus Runway, McMurdo Station, Antarctica. Geophysics, Vol.61(6), pp.1653-1663.

ASTM Standard Designation, D 6432 – 99 (Reapproved 2005) Standard Guide for Using the Surface Ground Penetrating Radar Method for Subsurface Investigation.

Bakker, M., 2004. The internal structures of Pleistocene push moraines – PhD Thesis, Queen Mary College, Univ. of London. Published by TNO Netherlands, 177 p.

Bristow, C. S. and Jol, H. M., 2003. Ground Penetrating Radar in Sediments. Geological Society London Special Publication, 211.

Coon, J. B., Fowler, J. C. and Schafers, C .J., 1981. Experimental uses of short pulse radar in coal seams. Geophysics, Vol.46, pp.1163-1168.

Cristina, Pauselli; Costanzo, Federico; Alessandro, Frigeri; Roberto, Orosei; Massimiliano, R. Barchi and Gabriele, Basile, 2010. Ground penetrating radar investigations to study active faults in the Norcia Basin (central Italy). Journal of Applied Geophysics, Vol.72, pp.39-45.

Daniels, J. J.; Brower, J. and Baumgartner, F., 1998. High resolution GPR at Brookhaven National Laboratory to delineate complex subsurface targets. Journal of Environmental and Engineering Geophysics, Vol.3(1), pp.1-5.

David, F. D.; Kathleen, Egan; Cindy, Carney; Paul, J. W. and Mark, R. B., 1995. Delineation of shallow stratigraphy using ground penetrating radar. Journal of Applied Geophysics, Vol.33, pp.167-175.

Davis, J. L. and Annan, A. P., 1989. Ground penetrating radar for high-resolution mapping of soil and rock stratigraphy. Geophysical prospecting, Vol.37, pp.531-551.

Day-Lewis, F. D.; Lane, J. W.; Harris, J. M. and Gorelick, S. M., 2003. Time-lapse imaging of saline tracer transport in fractured rock using difference radar attenuation tomography. Water Resources Research, Vol.39, 1290 p., doi: 10.1029/2002WR001722.

Derald, G. S. and Harry, M. J., 1995. Ground penetrating radar: antenna frequencies and maximum probable depths of penetration in Quaternary sediments. Journal of Applied Geophysics, Vol.33, pp.93-100.

Evans, D. L.; Farr, T. G.; Van, Z. J. J. and Zebker, H. A., 1988. Radar Polarimetry: Analysis Tools and Applications. IEEE Transactions on Geoscience and Remote Sensing, Vol.26(6), pp.774-789.

Fengshou, Zhang; Xiongyao, Xie and Hongwei, Huang, 2010. Application of ground penetrating radar in grouting evaluation for shield tunnel construction. Tunnelling and Underground Space Technology, Vol.25, pp.99-107.

Francke, J. and Yelf, R., 2003. Applications of GPR for Surface Mining: Proc. of the 2nd International Workshop on Advanced GPR. A Yarovoy (ed.) Published by IEEE (International Research Centre for Tele communications and Radar, Delft University, Netherlands), pp.115-119.

Fullagar, P. K.; Livelybrooks, D. W.; Zhang, P. and Calvert, A. J., 2000. Radio tomography and borehole radar delineation of the McConnell nickel sulphide deposit, Sudbury, Ontario. Canada : Geophysics, Vol.65, pp.1920-1930.

Grandjean, G.; Gourry, J. C. and Bitri, A., 2000. Evaluation of GPR techniques for civil-engineering applications: study on a test site. Journal of Applied Geophysics, Vol.45, pp.141-156.

Gross, R.; Holliger, K.; Green, A.; Seitz, G. and Baldwin, J., 1999. 3D Ground Penetrating Radar on the San Andreas Fault: A Complementary Paleoseismological Tool, abstract, AGU Fall Meeting.

Gross, Ralf; Holliger, Klaus; Alan, G. G. and Begg, John., 2000. 3D ground penetrating radar applied to paleoseismology : examples from the Wellington Fault, New Zealand. Proceedings of SPIE Volume, 4084.

Hulsmeyer, C., 1904. German Patent No. 165546.

Jol, H. M. and Bristow, C. S., 2003. GPR in sediments: advice on data collection, basic processing and interpretation, a good practice guide. Geological Society of London, Special Publication, Vol.211, pp.9-27.

Jorge, A.; Avila-Olivera and Victor, H. Garduno-Monroy., 2008. A GPR study of subsidence-creep-fault processes in Morelia, Michoacán, Mexico; Engineering Geology, Vol.100, pp.69-81.

Kong, F. N. and Tore, L. B., 1995. Performance of a GPR system which uses step frequency signals. Journal of Applied Geophysics, Vol.33, pp.15-26.

Leimbach, G. and Lowy, H., 1910. German Patent No. 237944.

Mahmoudzadeh, M. R.; Frances, A.P.; Lubczynski, M. and Lambot, S., 2012. Using ground penetrating radar to investigate the water table depth in weathered granites - Sardon case study, Spain. Journal of Applied Geophysics, Vol.79, pp.17-26.

Moran, M. L.; Greenûeld, R. J.; Arcone, S. A. and Delaney, A. J., 2000. Multi dimensional GPR array processing using Kirchhoff migration. Journal of applied Geophysics, Vol.43(13), pp.281-295.

Morey, R. M., 1974. Continuous subsurface profiling by impulse radar. Proceedings of the Engineering Foundation Conference on Subsurface Exploration for Underground Excavation and Heavy Construction, pp.213-232.

Moysey, S. and Knight, R. J., 2004. Modelling the ûeld-scale relationship between dielectric constant and water content in heterogeneous systems. Water Resources Research, Vol.40, W03510, doi:10.1029/2003WR002589.

Mundher, Ali, Seger and Ahmed, Fouad, Nashait., 2000. Detection of Water-Table by Using Ground Penetration Radar. Eng. & Tech. Journal, Vol.29(3).

Olhoeft, G. R., 1988. Interpretation of Hole-to-Hole Radar Measurements. Proceedings of the Third Technical Symposium on Tunnel Detection, January 12-15, Golden, CO, pp.616-629.

Olhoeft, G.R., 2000. Maximizing the information return from ground penetrating radar. Journal of Applied Geophysics, Vol.43, pp.175-187

Olsson, O.; Falk, L.; Forslund, O.; Lundmark, L. and Sandberg, E., 1992. Borehole radar applied to the characterization of hydraulically conductive fracture zones in crystalline rock. Geophysical Prospecting, Vol.40, pp.104-116.

Ralston, C. J., 2000. Use of Ground Penetrating Radar in underground coal mining, in Proceedings of 8th International Conference on GPR, pp.731-736.

Rubin, L. A. and Fowler, J. C., 1978. Ground-probing radar for delineation of rock features. Engineering Geology, Vol.12, pp.163-170.

Salvi, S.; Cinti, F. R.; Colini, L.; D'Addezio, G.; Doumaz, F. and Pettinelli, E., 2003. Investigation of the active Celano–L'Aquila fault system, Abruzzi (central Apennines, Italy) with combined ground penetrating radar and palaeoseismic trenching. Geophys. J. Int., Vol.155, pp.805-818.

Sheng-Huoo, Ni.; Yan-Hong, Huang; Kuo-Feng, Lo. and Da-Ci, Lin., 2010. Buried pipe detection by ground penetrating radar using the discrete wavelet transform. Computers and Geotechnics, Vol.37, pp.440-448.

Tetsuma, Toshioka; Tsuneo, Tsuchida and Katsuo, Sasahara., 1995. Application of GPR to detecting and mapping cracks in rock. Journal of Applied Geophysics, Vol.33, pp.119-124.

Thierbach, R., 1974. Electromagnetic reûections in salt deposits. Journal of Geophysics, Vol.40, pp.633-637.

Tronicke, J. and Holliger, K., 2004. Effects of gas- and water-ûlled boreholes on the amplitudes of crosshole georadar data as inferred from experimental evidence. Geophysics, Vol.69, pp.1255-1260.

Ulriksen, C. P., 1982. Application of impulse radar to civil engineering. Published Ph.D. Thesis, Lund University of Technology, Lund, Geophysical Survey Systems, Inc. Hudson, New Hampshire, pp.175-179.

Unterberger, R. R., 1978. Radar Propagation in Rock Salt. Geophysics Prospect, Vol.26, pp.312-328.

Veeken, P. C. H.; Dagallier, G.; Malartre, F.; Laitinen, A. L. and Van, Campenhout, L. P. A. M., 1999. Application of digital ground penetrating radar (GPR) for investigating the geology and structuration of the shallow subsurface. Proceedings of the 13th annual international conference on applied geologic remote sensing: Vancouver, B. C., Canada, pp.II-419-II-429.

Walford, M., 1985. Exploration of temperate glaciers. Physics Bulletin, Vol.36, pp.108-109.

Xingxin, Xu.; Qiaosong, Zeng; Dong, Li.; Jin, Wu; Xiangan, Wu and Jinyin, Shen, 2010. GPR detection of several common subsurface voids inside dikes and dams. Engineering Geology, Vol.111, pp.31-42.

Yetton, M. D. and Nobes, D. C., 1998. Recent vertical offset and near-surface structure of the Alpine Fault in Westland, New Zealand, from ground penetrating radar profiling: New Zealand. Journal of Geology and Geophysics, Vol.41, pp.485-492.